

Published in final edited form as:

*Biochem Biophys Res Commun.* 2014 January 3; 443(1): 110–114. doi:10.1016/j.bbrc.2013.11.073.

## The Cataract-associated V41M<sup>1</sup> mutant of human $\gamma$ S-crystallin shows specific structural changes that directly enhance local surface hydrophobicity<sup>2</sup>

Somireddy Venkata Bharat, Alexander Shekhtman, and Jayanti Pande\*

Department of Chemistry, University at Albany, State University of New York, Albany, N.Y., 12222

### Abstract

The major crystallins expressed in the human lens are  $\gamma$ S-,  $\gamma$ C- and  $\gamma$ D-crystallins. Several mutations in  $\gamma$ S-crystallin are associated with hereditary cataracts, one of which involves the substitution of a highly conserved Valine at position 41 to Methionine. According to a recent report, the mutant protein, V41M, shows lower stability and increased surface hydrophobicity compared to the wild-type, and a propensity for self-aggregation. Here we address the structural differences between the two proteins, with residue-level specificity using NMR spectroscopy. Based on the structural model of the mutant protein, our results clearly show that the mutation creates a major local perturbation almost at the junction of the first and second “Greek-key” motifs in the N-terminal domain. A larger section of the second motif (residues 44–86) appears to be mainly affected. Based on the large chemical shift of the imino proton of the indole side-chain of Trp46 in the mutant protein, we suggest that the sulphur atom of Met41 is involved in an S– $\pi$  interaction with Trp46. This interaction would bring the last  $\beta$ -strand of the first “Greek-key” motif closer to the first  $\beta$ -strand of the second motif. This appears to lead to a domino effect, towards both the N- and C-terminal ends, even as it decays off substantially beyond the domain interface. During this process discreet hydrophobic surface patches are created, as revealed by ANS-binding. Such changes would not affect the secondary structure or cause a major change in the tertiary structure, but can lead to self-aggregation or aberrant binding interactions of the mutant protein *in vivo*, and lead to lens opacity or cataract.

### Keywords

crystallin; cataract; hydrophobicity; NMR spectroscopy; S– $\pi$  interactions

<sup>1</sup>**Abbreviations:** HGS, Human  $\gamma$ S crystallin; V41M, the Val41Met mutant of human  $\gamma$ S crystallin; HSQC, Heteronuclear single quantum coherence; ANS, 8-Anilino-naphthalene-1-sulfonic acid; Bis-ANS, 4,4'-Dianilino-1,1'-binaphthyl-5,5' disulfonic acid; CSP, Chemical shift perturbation

<sup>2</sup>The same mutant has also been called V42M by counting the start-codon as residue 1, but Val is the 41<sup>st</sup> residue of the protein.

© 2013 Elsevier Inc. All rights reserved.

\*Corresponding author. Address: Department of Chemistry, Life Sciences Research Building, University at Albany, State University of New York, 1400 Washington Avenue, Albany, N.Y., 12222, jpande@albany.edu.

**Publisher's Disclaimer:** This is a PDF file of an unedited manuscript that has been accepted for publication. As a service to our customers we are providing this early version of the manuscript. The manuscript will undergo copyediting, typesetting, and review of the resulting proof before it is published in its final citable form. Please note that during the production process errors may be discovered which could affect the content, and all legal disclaimers that apply to the journal pertain.

## 1. Introduction

In the human ocular lens  $\gamma$ S-crystallin (HGS) is a highly expressed member of the  $\gamma$ -crystallin family along with  $\gamma$ C- and  $\gamma$ D-crystallins [1]. Several point mutations of  $\gamma$ S-crystallin have been associated with hereditary cataracts [2,3,4,5]. The V41M mutation in  $\gamma$ S-crystallin has been shown to be associated with congenital, autosomal-dominant, bilateral cataract in three generations of a northern Indian family [5]. Our previous studies with the cataract-associated mutants of human  $\gamma$ D-crystallin [6,7,8], have shown that a comparison of the structure and solution properties of the mutant protein with those of the wild-type *in vitro* provide a compelling rationale for the molecular basis of the disease. Recent studies by Vendra et al [9] *in vitro* on the V41M mutant of HGS showed several distinguishing properties between the wild-type and mutant proteins: Specifically, the mutant protein showed lower stability in thermal and chemical denaturation experiments, a propensity for aggregation, and a red-shifted Trp fluorescence emission spectrum – even as the secondary structure, and to a large extent, the tertiary structure appeared to be unaltered. Here we identify the structural differences between the two proteins at the residue-level using NMR spectroscopy, and suggest how these differences are likely to affect the properties of the mutant.

## 2. Experimental Methods

### 2.1 Protein Expression and Purification

Human  $\gamma$ S cDNA cloned in pET3a vector was a generous gift from Dr. Nicolette Lubsen (Radboud University, Nijmegen, The Netherlands). Mutation of Val 41 was carried out using the Quickmut site-directed mutagenesis kit from Agilent, and the following forward primer:

5'-GCAACTCCATTAATAATGGAAGGAGGCACCTGG-3', and its reverse complement. Procedures for protein expression and purification were almost identical as for human  $\gamma$ D-crystallin [6]. Briefly, *E. coli* (BL21 (DE3)) cells were grown at 37°C to an absorbance of ~0.7. The protein was overexpressed by induction with isopropyl  $\beta$ -D-1-thiogalactopyranoside (IPTG) at a final concentration of 1mM. U-<sup>15</sup>N labeled protein was produced in M9 minimal medium with <sup>15</sup>NH<sub>4</sub>Cl as the sole nitrogen source. For the <sup>13</sup>C labeled proteins U-<sup>13</sup>C-glucose was used as the carbon source. Cell pellets were lysed in a buffer containing 5 mM Tris-HCl, pH 8, 25 mM NaCl, 2 mM EDTA, 1 tablet protease inhibitor (Roche biochemical) and lysozyme (250  $\mu$ g/ml). Five cycles of rapid freeze-thaw procedure was carried out by rapid freezing in liquid nitrogen and thawing in water at 30°C. The lysate was incubated with 25  $\mu$ g/mL DNase (Sigma) followed by centrifugation at 48,000  $\times$  g, to collect the supernatant. The supernatant contained over 90% of the protein.

Purification of the wild-type HGS and the V41M mutant (V41M) was carried in two steps, first using size-exclusion chromatography, followed by cation-exchange chromatography [10]. Electrospray Ionization Mass Spectroscopy analysis, performed at the UAlbany Proteomics Facility, gave a mass of 20,875  $\pm$  1 Da for different preparations of the wild-type, and 20,916.5  $\pm$  0.5 for various preparations of the V41M mutant. The “theoretical” masses computed from the protein sequences ([www.expasy.ch](http://www.expasy.ch)) are 20,875 for the wild-type and 20,918 for the V41M mutant.

### 2.2 NMR sample preparation

The protein concentrations of [<sup>15</sup>N] HGS and V41M were determined from the absorbance at 280 nm ( $\epsilon = 42,860 \text{ M}^{-1} \text{ cm}^{-1}$ , ([www.expasy.ch](http://www.expasy.ch))). For the NMR experiments, sample concentrations ranging between 0.3 – 0.6 mM in 100 mM Phosphate buffer, pH 6.0, 0.05% sodium azide with or without 20 mM DTT, and 10% D<sub>2</sub>O were used.

### 2.3 NMR experiments

All NMR spectra were recorded at 298 K on a Bruker Avance 700 MHz spectrometer, equipped with a z-axis gradient TXI cryoprobe. Assignments of the  $^{15}\text{N}$  and  $^1\text{H}$  nuclei of HGS were aided by known literature assignments [11,12]. The backbone amide protons of both wild type and mutant HGS were assigned by using 2D [ $^1\text{H}$ ,  $^{15}\text{N}$ ] HSQC and triple resonance experiments, CBCACONH and HNCA [13]. The data were processed by using Topspin 2.1 (Bruker, Inc) and analysed by using CARA software [14]. Ser 1, Lys 2, Tyr 59, Ser 89, Lys 94, and Val 131–135, Gln 148, Asp 152-Lys 154, and Tyr 156 were unassigned due to signal broadening. The Chemical shift perturbations of  $^{15}\text{N}$  and  $^1\text{H}$  nuclei between HGS and V41M were analyzed by overlaying the spectra of [ $U$ - $^{15}\text{N}$ ] HGS and V41M (Fig 1). The average chemical shift perturbations (CSP),  $\Delta\delta_{\text{avg}}$ , were calculated according to the Eq. 1.1.

$$\Delta\delta_{\text{avg}} = \sqrt{\frac{(\Delta\delta^{\text{N}}/5)^2 + (\Delta\delta^{\text{H}})^2}{2}} \quad (1.1)$$

where  $\Delta\delta_{\text{N}}$  and  $\Delta\delta_{\text{H}}$  are the chemical shift perturbations of the amide nitrogen and amide proton, respectively.

### 2.4 ANS-binding studies

Binding of the ammonium salt of 8-Anilino-naphthalene-1-sulfonic acid (ANS) to HGS and V41M mutant was first monitored using fluorescence emission at 500nm ( $\lambda_{\text{ex}}$  at 390nm) using an ANS: protein molar ratio of 5, in 0.1 M phosphate buffer at pH 7. Emission intensity of the mutant was more than double that of the wild-type protein (data not shown). After establishing that the fluorescence increase for the V41M mutant compared to the wild-type was substantial, [ $^{15}\text{N}$ ,  $^1\text{H}$ ] HSQC were conducted using [ $U$ - $^{15}\text{N}$ ] HGS and V41M. Protein concentration was 0.25 mM and the final molar ratio of 1:5 (protein: ANS).

### 2.5 Molecular modeling

The 3D structure of V41M was obtained by homology-modeling, using the NMR structure of the mouse  $\gamma\text{S}$ -crystallin (PDB ID: 2A5M) as the template. The automated modeling mode of SwissModel (swissmodel.expasy.org) was used. The models were analyzed by using Pymol software ([www.pymol.org](http://www.pymol.org)).

## 3. Results and Discussion

In Fig. 1, the [ $^{15}\text{N}$ ,  $^1\text{H}$ ] HSQC spectrum of [ $U$ - $^{15}\text{N}$ ] HGS is overlaid with that of the [ $U$ - $^{15}\text{N}$ ] V41M mutant. Our assignments agree with those of Baraguey *et al.*, [11] at pH 6, and Brubaker *et al.*, [12] at pH 4.5. It should be noted, however, that Brubaker *et al.*, had an additional N-terminal Gly residue in HGS, and Baraguey *et al.*, used the Cys24Ser mutant instead of HGS.

The main feature readily observed in Fig. 1 are the large chemical shift perturbations (CSPs) in the main chain amides of residues close to the mutation site, namely Glu42, Gly43, Gly44, Thr45 and Trp46. Residues with large chemical shift perturbation ( $< 0.1$  ppm) between the two proteins are marked by a circle and their shifts indicated by arrows. One can also see the shifts in the main chain amides of residues 64 to 66. These two clusters of residues (42 to 46 and 63–66) show maximum CSP (which is also clearly shown in Fig. 2 discussed below). We also observe a remarkable shift in the side chain of W46 (W46 $\epsilon$  in the lower-left corner), while the side-chains of the remaining three tryptophan residues do not show any significant corresponding shift.

Fig. 2 shows a plot of the observed CSP for each residue drawn from the HSQC data in Fig. 1. The maximum perturbation is observed in residues near the mutation site (see E42 and G44) in the first “Greek key” motif (residues 5 to 43) of the N-terminal domain, followed by the residues 45 to 49 which form the first strand of the second “Greek-key” motif (residues 44–86) which are also significantly perturbed. Furthermore, residues belonging to the adjacent two strands, i.e. residues 60 to 66 (see Inset, green thick spaghetti) show high perturbation. Beyond these clusters of residues that are mainly affected, we note that residues 7–8, 22–23, and 84–85 show minor perturbation, and all belong to different  $\beta$ -strands. Remarkably, residues belonging to the “Greek-key” motif 3 (cyan), namely residues 93–133 are totally unaffected since this motif is far removed from the perturbed strands. Thus the overall effect of mutation appears to be transmitted in a discreet pattern and leads us to propose that the perturbation is transmitted away from the mutation-site primarily by strand-strand interactions.

As pointed out earlier, in addition to a large CSP in the main chain amide of Trp 46, we also observed a large shift in the side chain imine of the Trp 46 indole. In our molecular model of HGS (Fig. 2, inset), the distance between Met41 and the centre of the benzene ring of indole in Trp 46 is about 6.5 Å. It has been suggested that the energy associated with such Met-S- $\pi$  interactions is about 1–3 kcal/mole [15]. Since residue 41 and 46 are in adjoining beta-strands such an interaction is likely to perturb the inter-strand distance and/or orientation between these strands. Furthermore, Tyr66 is almost at the same distance from the Met41-S atom as Trp46 on the opposite side and a part of another strand. If indeed the Met-S- $\pi$  interaction is also occurring with Tyr 66, it would explain why the cluster of residues 61–66 shows higher perturbation. Valley *et al.*, [15] have provided many examples from the PDB database of protein structures in which a Met residue interacts with 2 or more aromatic amino acids. They also provide examples in which substitution of a Met making S- $\pi$  interactions in the wild-type protein with another residue results in dramatically altering the enzymatic or biochemical activity. Therefore, we suggest that the Met41-S- $\pi$  interactions may be playing a key role in affecting the structural changes we observe in the V41M mutant of HGS.

We should point out that our NMR data are analysed on the basis of a homology-model based on the NMR structure [16] of mouse  $\gamma$ S-crystallin (PDB ID: 2A5M). Since 90% of the residues in the human protein are identical to those in the mouse protein, we believe that our model is reliable.

Vendra *et al* [9] have already shown that the bis-ANS complex of the V41M mutant shows much higher emission than wild-type HGS. However, we wanted to determine the binding site(s) for the dye, using NMR. Due to the low solubility of bis-ANS-V42M- $\gamma$ S complex, we used the ANS dye instead, which showed fluorescence enhancement similar to that of bis-ANS. Fig. 3 shows the CSP due to ANS binding to HGS and the mutant. A horizontal line corresponding to the CSP of 0.005 has been drawn in panels B and C as an arbitrary cut-off, such that the CSP values above the cut-off are considered significant. Since the data in panels B and C are plotted using identical scales, it is clear that the CSPs, particularly in the N-terminal domain, are significantly higher for the mutant (panel C) than for the wild type — specifically with residues clustered around residue 20 and residue 60, and also individual residues E42, W72, G91 and C129.

$\gamma$ S-crystallin is a unique member of the  $\gamma$ -crystallin family, since its presence slows the formation of disulphide-linked aggregates of other  $\gamma$ -crystallins [17] and it also reduces the phase-separation temperature in mixtures with other  $\gamma$ -crystallins [18]. Thus, overall it appears to play an important role in suppressing the formation of light-scattering elements and maintaining lens transparency. The structural perturbations in the mutant V41M

described above, could override the original, protective properties of HGS, which allow it to suppress the formation of such light-scattering elements. The effects of the V41M mutation on the other properties of  $\gamma$ S-crystallin are currently being investigated.

## Acknowledgments

We are grateful to Dr. N. Lubsen for the gift of the cDNA clone for human  $\gamma$ S crystallin. Dr. Ajay Pande prepared the V41M mutant and confirmed its correct expression. He also built the molecular model for the mutant protein, and participated in drawing figures 2 & 3, and in writing the manuscript. This work was supported by NIH grants GM085006 to A.S. and EY010535 to J.P

## References

1. Siezen RJ, Thomson JA, Kaplan ED, Benedek GB. Human lens gamma-crystallins: isolation, identification, and characterization of the expressed gene products. *Proc Natl Acad Sci U S A.* 1987; 84:6088–6092. [PubMed: 3476929]
2. Devi RR, Yao W, Vijayalakshmi P, Sergeev YV, Sundaresan P, Hejtmancik JF. Crystallin gene mutations in Indian families with inherited pediatric cataract. *Mol Vis.* 2008; 14:1157–1170. [PubMed: 18587492]
3. Sun H, Ma Z, Li Y, Liu B, Li Z, Ding X, Gao Y, Ma W, Tang X, Li X, Shen Y. Gamma-S crystallin gene (CRYGS) mutation causes dominant progressive cortical cataract in humans. *J Med Genet.* 2005; 42:706–710. [PubMed: 16141006]
4. Sun W, Xiao X, Li S, Guo X, Zhang Q. Mutation analysis of 12 genes in Chinese families with congenital cataracts. *Mol Vis.* 2011; 17:2197–2206. [PubMed: 21866213]
5. Vanita V, Singh JR, Singh D, Varon R, Sperling K. Novel mutation in the gamma-S crystallin gene causing autosomal dominant cataract. *Mol Vis.* 2009; 15:476–481. [PubMed: 19262743]
6. Pande A, Pande J, Asherie N, Lomakin A, Ogun O, King JA, Lubsen NH, Walton D, Benedek GB. Molecular basis of a progressive juvenile-onset hereditary cataract. *Proc Natl Acad Sci U S A.* 2000; 97:1993–1998. [PubMed: 10688888]
7. Pande A, Ghosh KS, Banerjee PR, Pande J. Increase in surface hydrophobicity of the cataract-associated P23T mutant of human gammaD-crystallin is responsible for its dramatically lower, retrograde solubility. *Biochemistry.* 2010; 49:6122–6129. [PubMed: 20553008]
8. Banerjee PR, Pande A, Patrosz J, Thurston GM, Pande J. Cataract-associated mutant E107A of human gammaD-crystallin shows increased attraction to alpha-crystallin and enhanced light scattering. *Proc Natl Acad Sci U S A.* 2011; 108:574–579. [PubMed: 21173272]
9. Vendra VP, Chandani S, Balasubramanian D. The mutation V42M distorts the compact packing of the human gamma-S-crystallin molecule, resulting in congenital cataract. *PLoS One.* 2012; 7:e51401. [PubMed: 23284690]
10. Broide ML, Berland CR, Pande J, Ogun OO, Benedek GB. Binary-liquid phase separation of lens protein solutions. *Proc Natl Acad Sci U S A.* 1991; 88:5660–5664. [PubMed: 2062844]
11. Baraguey C, Skouri-Panet F, Bontems F, Tardieu A, Chassaing G, Lequin O. (1)H, (15)N and (13)C resonance assignment of human gammaS-crystallin, a 21 kDa eye-lens protein. *J Biomol NMR.* 2004; 30:385–386. [PubMed: 15754064]
12. Brubaker WD, Martin RW. (1)H, (1)(3)C, and (1)(5)N assignments of wild-type human gammaS-crystallin and its cataract-related variant gammaS-G18V. *Biomol NMR Assign.* 2012; 6:63–67. [PubMed: 21735120]
13. Cavanagh, J. *Protein NMR spectroscopy: principles and practice.* 2. Academic Press; Amsterdam; Boston: 2007.
14. Masse JE, Keller R. AutoLink: automated sequential resonance assignment of biopolymers from NMR data by relative-hypothesis-prioritization-based simulated logic. *J Magn Reson.* 2005; 174:133–151. [PubMed: 15809181]
15. Valley CC, Cembran A, Perlmutter JD, Lewis AK, Labello NP, Gao J, Sachs JN. The methionine-aromatic motif plays a unique role in stabilizing protein structure. *J Biol Chem.* 2012; 287:34979–34991. [PubMed: 22859300]

16. Grishaev A, Wu J, Trehella J, Bax A. Refinement of Multidomain Protein Structures by Combination of Solution Small-Angle X-ray Scattering and NMR Data. *Journal of the American Chemical Society*. 2005; 127:16621–16628. [PubMed: 16305251]
17. Liu C, Pande J, Lomakin A, Ogun O, Benedek GB. Aggregation in aqueous solutions of bovine lens gamma-crystallins: special role of gamma(s). *Invest Ophthalmol Vis Sci*. 1998; 39:1609–1619. [PubMed: 9699550]
18. Liu C, Asherie N, Lomakin A, Pande J, Ogun O, Benedek GB. Phase separation in aqueous solutions of lens gamma-crystallins: special role of gamma s. *Proc Natl Acad Sci U S A*. 1996; 93:377–382. [PubMed: 8552642]

**HIGHLIGHTS**

- We present NMR analysis of V41M, a cataract-causing mutant of human  $\gamma$ S-crystallin.
- Mutation alters strand-strand interactions throughout the N-terminal domain.
- Mutation directly affects Trp46 due to key Met41-S-Trp46- $\pi$  interactions.
- We identify the basis of the surface hydrophobicity increase and residues involved.

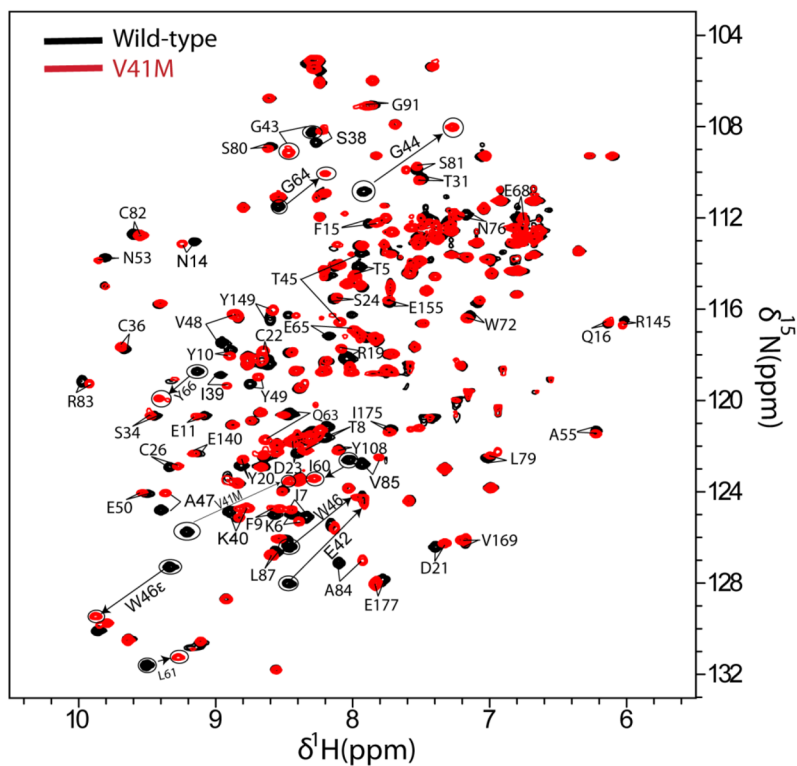


**Figure 1.**  
 2D  $^{15}\text{N}$ - $^1\text{H}$  HSQC spectrum of [ $U$ -, $^{15}\text{N}$ ] HGS (black contours), overlaid with [ $U$ -, $^{15}\text{N}$ ] V41M mutant (red contours), in 100 mM PBS buffer, pH 6.0. Residues with large average chemical shift perturbation ( $< 0.1$  ppm) between the two proteins are marked by a circle and their shifts indicated by arrows. Large shifts in residues close to the mutation site, namely E42, G43, G44, T45 and W46 are clearly depicted – see also Fig. 2. The shift in the side chain of W46 (W46e in the lower-left corner) is also observed, while the remaining three tryptophan residues do not show a significant corresponding shift.

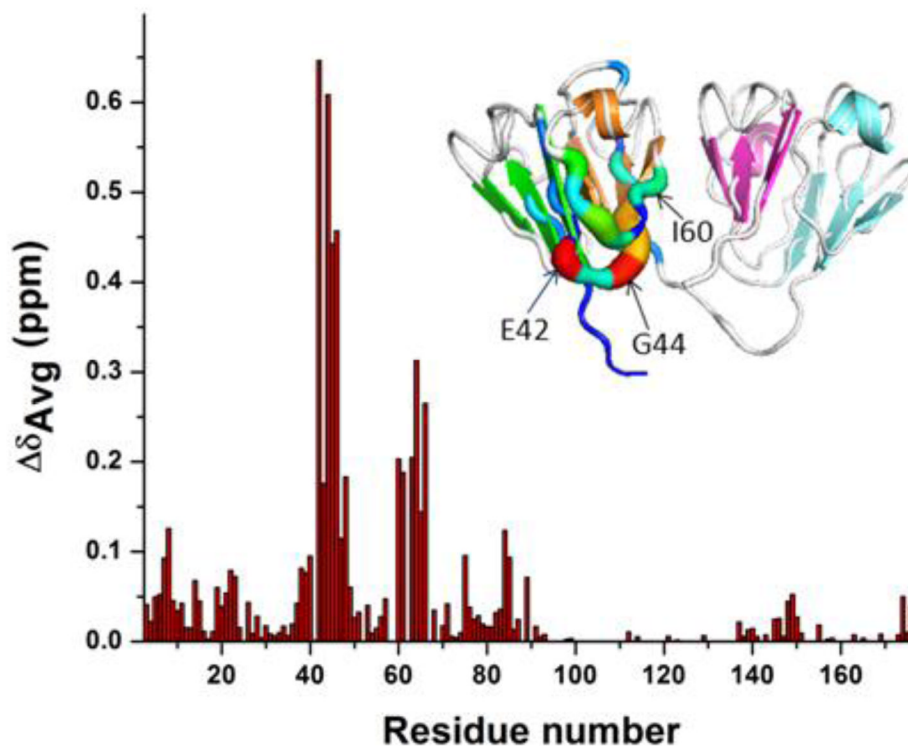


**Figure 2.**

Averaged amide chemical shift perturbation (CSP) between the mutant V41M and the wild-type HGS. *Inset* shows a model of the mutant on which the CSPs are mapped as a “putty” using Pymol (Delano Scientific). The highest value of CSP is shown in red and lowest in blue, with radius of the ribbon also increasing from low CSP to high CSP. The secondary structural elements (strands and helices) are superimposed on the ribbon-putty, and are coloured according to the “Greek-key” motifs they belong to: i.e. green, orange, cyan and magenta for motifs 1 to 4 respectively. The maximum perturbation is observed in residues near the mutation site (see E42 and G44) in the first “Greek key” motif (residues 5 to 43) of the N-terminal domain. Residues 45 to 49, forming the first strand of the second “Greek-key” motif are also significantly perturbed. Residues 60 (see Inset) to 66 (green thick spaghetti) also show high perturbation, as they are adjacent to residues 42 and 44. Clearly the structure of the second motif (residues 44 to 86) of the N-terminal domain is substantially perturbed. On the other hand, motif 3 (cyan) containing residues 93–133 is totally unaffected as it is far removed from the mutation site. Residues on either end of the mutation site are affected, but the effect appears to be transmitted in a discreet pattern, probably propagated by strand-strand interaction. Residues 148 to 150 and 174–175 are part of two adjacent strands, which show minimal perturbation in motif 4. Overall, it appears that the perturbation is largely carried over from the mutation site by strand-strand interactions.

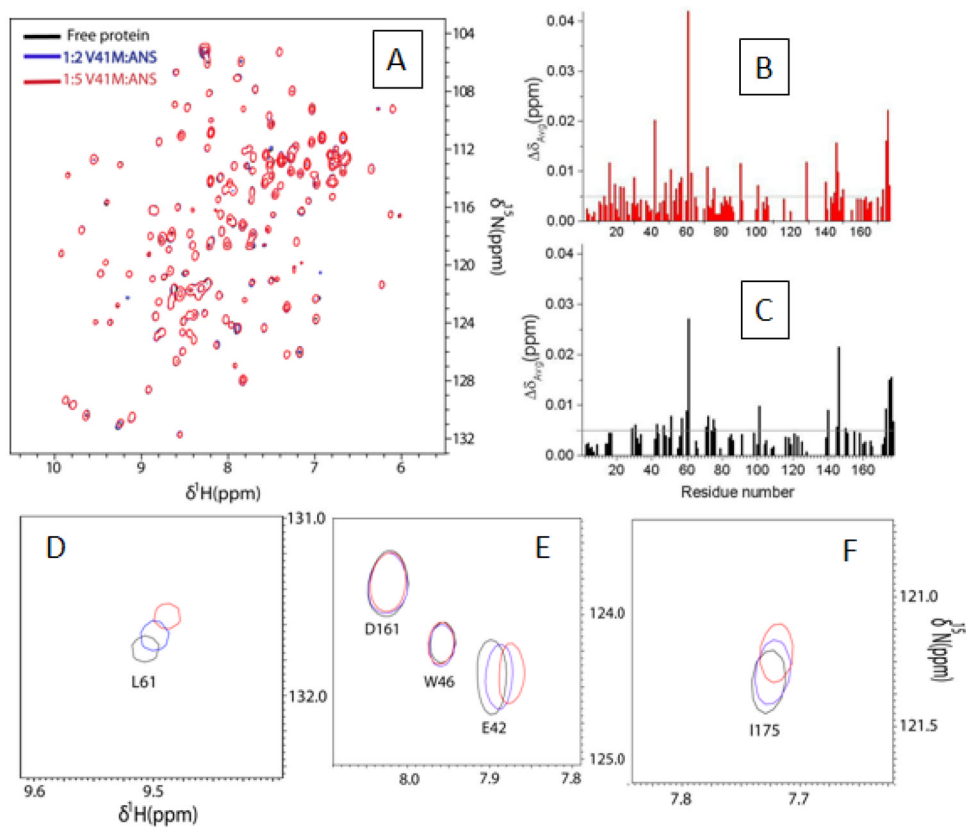


**Figure 3.** Amide chemical shift perturbations (CSP) in the  $^{15}\text{N}$ - $^1\text{H}$  HSQC spectrum of  $[U-, ^{15}\text{N}]$  V41M (black contours), due to ANS binding (A); CSP in the presence of 5X molar excess of ANS (data from panel A) in  $[U-, ^{15}\text{N}]$  V41M mutant (B. ); CSP in the presence of 5X molar excess of ANS (data not shown) in  $[U-, ^{15}\text{N}]$  HGS (C). A horizontal line corresponding to the CSP of 0.005 has been drawn in panels B and C as an arbitrary cut-off for a significant CSP. Since the data in panels B and C are plotted using identical scales, it is clear that the CSPs, particularly in the N-terminal domain, are significantly higher for the mutant (panel C); specifically, residues clustered around residue 20 and residue 60, and individual residues E42, W72, G91 and C129. In panels D, E, and F CSPs of L61, E42 and I175 respectively, are shown in an expanded scale. Only one contour per residue is shown for clarity.